Chapter 4

Imaging of refractive index distribution in phase objects

4.1 Introduction

Digital holography is an imaging modality reconstructing directly the wavefront from a single digitalized hologram in a numerical form. It brings quantitative data derived simultaneously from the amplitude and phase of the complex reconstructed wavefront diffracted by the object and it can be used to determine the refractive index and/or shape of the object with high accuracy. Since numerical reconstruction provides both the amplitude and phase of the wavefronts it finds immense potential applications ranging from shape measurement to microscopy. The method is useful especially for phase objects, which otherwise does not produce any change in the amplitude of the interacting wavefront and hence is difficult to image. The wavefronts passing through a region having non-uniform refractive index distribution will carry the information about this distribution as a spatially varying phase. Digital holography can be used for measurement of this phase.

Phase objects cannot be imaged directly since they do not produce any variation to the amplitude of the wavefront interacting with them. But since they introduce a change in optical path length and hence phase of this wavefront, phase objects could be characterized by measuring the phase changes occurring to this wavefront. Refractive index distribution existing inside such an object produces a spatial variation in the phase of the wavefront passing through the object. The refractive index in turn depends upon many local parameters of interest such as density, temperature, impurity distribution etc. So a measurement of the refractive index distribution could be used to map these parameters. These type of objects include any gaseous systems, temperature distributions produced by flames, plasmas etc. The measurement and mapping of these parameters with fine spatial and temporal resolution is of primary interest to any one working in these fields [4.1-4.4].

Many optical techniques can be used to map the refractive index profile. This includes the shadow, schlieren and interferometric techniques. Each of these methods yields the second derivative of refractive index profile, derivative of refractive index and the refractive index respectively [4.3]. So interferometric methods definitely have an advantage over the other two even though it is has to satisfy stringent optical conditions. Interferometric methods especially holography and holographic interferometry could be used to determine the refractive index distributions [4.3-4.9]. Digital holograms can be reconstructed numerically using scalar diffraction theory yielding the complex amplitude of the object wavefront [4.10, 4.11]. The phase of the object wavefront can be calculated from the complex amplitude. In this chapter the use of holographic interferometry in investigating axi-symmetric refractive index fields existing in various phase objects like flames and transparent dielectric mediums subjected to heating is described [4.12].

4.2 Experimental setup and hologram reconstruction

Fig. 4.1 shows the experimental setup used to record the digital holograms of the phase objects for mapping their refractive index distributions. A Mach-Zehnder interferometric setup was employed. In the present situation the investigated systems were not transient in nature, so continuous wave lasers were utilized. In all the cases the source used was a He-Ne laser.

The output from a He-Ne laser was split into two. The beams were expanded and collimated either individually. The object beam passes through the object under investigation. The object beam and the reference beam interfere at the CCD camera. The interferograms or holograms were recorded and stored in a PC for numerical reconstructions. For large objects a diffuser plate was placed just after the object, so that the whole of the object contributes to hologram recording. For objects with size of the order of the CCD chip the diffuser plate was removed.

Digital holograms were reconstructed either using Fresnel transform or Angular Spectrum Propagation integral depending on the situation. For large objects the use of diffuser plate entailed the use of Fresnel transform, where paraxial approximation is valid. For small objects and small propagation distances (CCD kept near the object) angular spectrum approach is used.

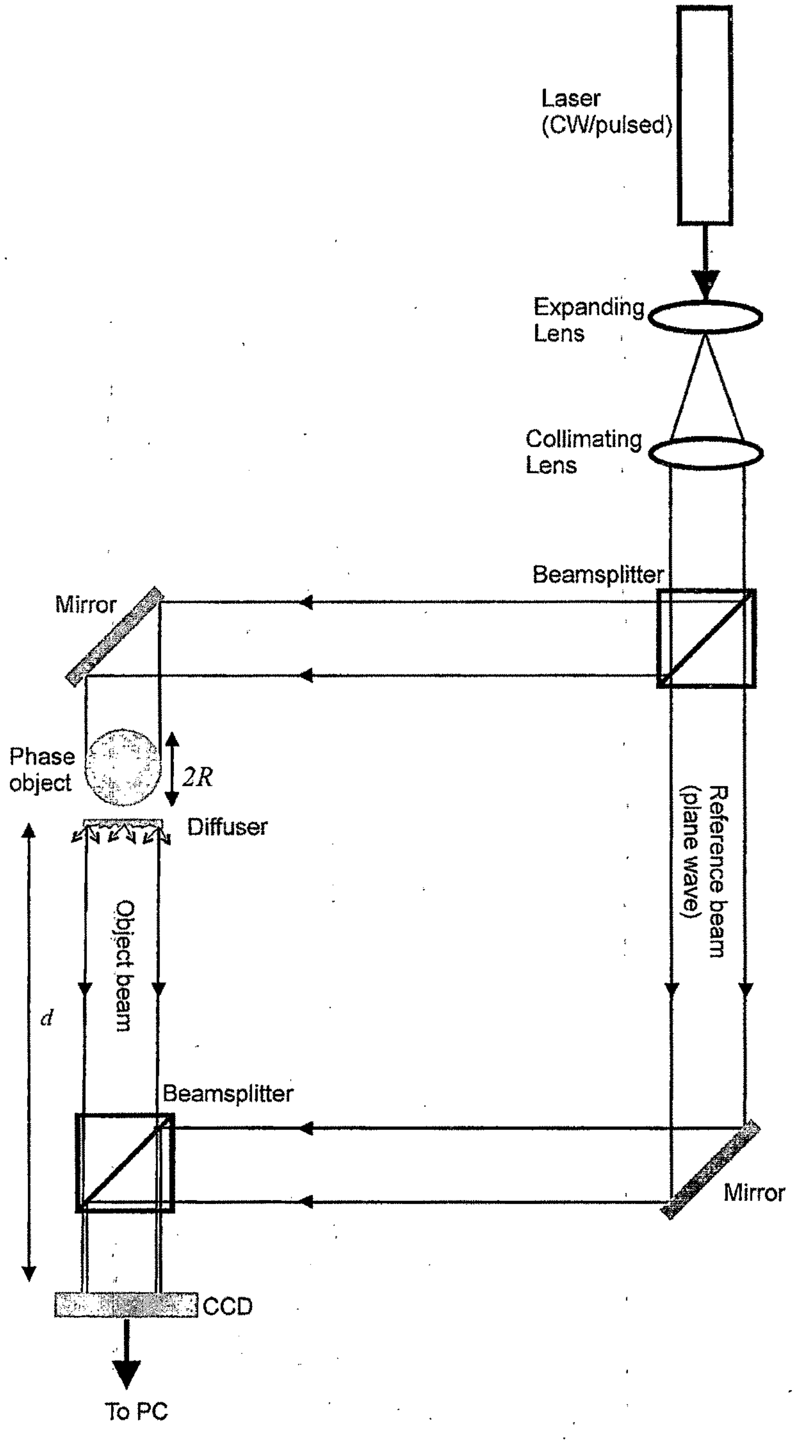

Fig. 4.1: Schematic of digital holography setup for imaging refractive index distributions in transparent objects.

Computer codes written in MATLAB for reconstruction of digital holograms using Fresnel transform and angular spectrum propagation integral were used for reconstructions and computation of interference phase.

4.3 Computation of phase difference

Both the Fresnel transform approach and the angular spectrum approach yields the complex amplitude of the object wavefront. Once the complex amplitude is available, the state or phase of the wavefront as well its intensity could be computed. The intensity of the wavefront is calculated from absolute square of the complex amplitude as

$$I(x,y)=\left|U(x,y)\right|^2 \tag{71}$$

and phase is calculated from the angle complex amplitude makes with the Real axis

$$\phi(x,y)=\arctan\frac{\mathrm{Im}\left[U(x,y)\right]}{\mathrm{Re}\left[U(x,y)\right]} \tag{72}$$

The phases of the two states of the object (without and with the refractive index distribution) are computed individually from the complex amplitudes of the two states $U_1(x, y)$ and $U_2(x, y)$. The phase difference provides information on the refractive index change occurring between the two object states. The phases of the individual sates can be written as

$$\phi_1(x,y)=\arctan\frac{\mathrm{Im}\left[U_1(x,y)\right]}{\mathrm{Re}\left[U_1(x,y)\right]} \tag{73}$$

$$\phi_2(x,y)=\arctan\frac{\mathrm{Im}\left[U_2(x,y)\right]}{\mathrm{Re}\left[U_2(x,y)\right]} \tag{74}$$

φ_1 is the phase of the object in the first (without the refractive index distribution) state and the φ_2 is phase for the second (with the refractive index distribution) state. The phase takes values between $-\pi$ and π.The interference phase (or phase difference) is now calculated directly by subtraction:

$$\begin{aligned}\Delta\phi(x,y) &= \phi_1(x,y)-\phi_2(x,y) \qquad \text{if } \phi_1>\phi_2 \\ &= \phi_1(x,y)-\phi_2(x,y)+2\pi \quad \text{if } \phi_2>\phi_1\end{aligned} \tag{75}$$

From this equation, we can calculate interference phase directly from the digital holograms. The resulting interference phase ranges from $-\pi$ to π and so was unwrapped before being used for finding the refractive index distributions.

4.4 Measurement of refractive index change

This phase difference acquired by a ray propagating in the z direction (Fig. 4.2) given in Eq. (75) is proportional to the refractive index change $\Delta n(x, y)$ according to

$$\Delta\phi(x,y)=\frac{2\pi}{\lambda}\int_{z_1}^{z_2}\left[n(x,y,z)-n_0\right]dz \tag{76}$$

where $n(x, y, z)$ is the position dependent refractive index inside the medium and n_0 is the constant refractive index of the medium before perturbation.

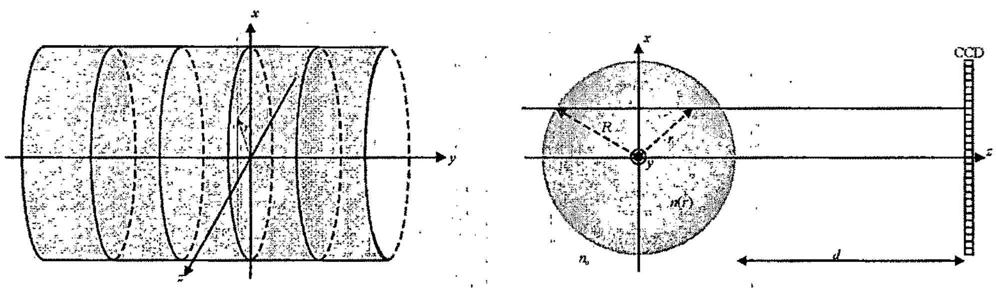

Fig. 4.2: Axi-symmetric refractive index distributions. (a) axi-symmetric phase object (b) The refractive index distribution at a particular (x, z) plane

The main interest is in the local values of refractive index change occurring in the medium. The obtained phase differences are chord integrated values or are due to the cumulative effect of the local refractive index changes occurring in the medium. An inversion of the chord integrated values represented by Eq. (76) is required to yield the local $n(x, y)$ values. This inversion of chord integrated values to yield local parameter of interest is called tomography. For axi-symmetrical phase objects the refractive index distribution is a function of r alone as shown in Fig. 4.2b [4.4, 4.8]. Several objects existing in nature have this type of refractive index distribution. This includes flames, transparent dielectric slabs exposed to point heat source, plasmas (especially laser produced), jets etc.

4.5 Abel Inversion

In Fig. 4.2 the light beam passes through the object in the z direction and the object is axi-symmetrical with respect to the y-axis. Then the refractive index at a particular (x, z) plane is a function of radius r alone. Eq. (76) could be modified to

$$\Delta\phi(x,y)=\frac{4\pi}{\lambda}\int_{x}^{R}\left[n(y,r)-n_0\right]\frac{rdr}{\sqrt{r^2-x^2}} \tag{77}$$

here $r=\sqrt{x^2+z^2}$

Eq. (77) is the Abel integral equation. This has an exact solution and its inversion will yield the values for the refractive index change and knowing n_0 the absolute position dependent refractive index can be determined.

$$n(y,r)-n_0=\Delta n(y,r)=\frac{\lambda}{2\pi^2}\int_{r}^{R}\frac{d\Delta\phi(x,y)}{dx}\frac{dx}{\sqrt{r^2-x^2}} \tag{78}$$

The inversion is achieved numerically by dividing the object into a number of annular regions with constant width inside which the refractive index is assumed to be a constant. So the tomographic problem involves solving a set of simultaneous linear algebraic equations. Since one has a discrete number of annular regions, the integral in Eq. (78) is replaced by a summation [4.3,4. 4,4. 8,4. 9].

4.6 Experimental Results

Experiments were conducted on several axi-symmetric objects. These objects included flames, temperature distribution in air by a point heat source and temperature distribution inside a dielectric slab due to a point heat source. The holograms of temperature distribution due to the point heat source in air were reconstructed using angular spectrum propagation method. The other two experiments used a diffuser after the phase object to image large area of the object. In these cases the CCD was kept at a large distance from the diffuser and Fresnel transform was used for the reconstructions. In all the cases holograms with and without the objects were recorded. The reconstructed phases with and with out the object was subtracted to yield the phase difference. This subtraction eliminates the changes occurring to the object wavefront due to aberrations of the optical elements as well as due to non-uniformity in the object due to reasons other than the refractive index change.

4.6.1 Refractive index distribution in a candle flame

First of the phase objects studied was a candle flame. A plane wavefront derived from a 611nm He-Ne laser (2mW, random linear polarization) was passed through the candle flame after it was lit. A CCD with 1024×1024 pixels having pixel size of 4.65μ×4.65μ and 8 bit dynamic range was kept 1.1m from the diffuser plate. Holograms were sampled at the rate of 1Hz and were reconstructed using the Fresnel transform method described in Section 7 of Chapter 2. Holographic interferomrtry in the case of digital holography can be achieved in two ways i) by supersposing the holograms and then doing the reconstruction and ii) by individually reconstructing the holograms and then applying a phase substraction. The first case yields the holographic interference fringes superposed on the image of the object as in the case of double exposure interferometry in convetional holography. Here once again a phase stepping is necessary to obtain the phase change occurring to object wavefront. In the second case the phase change is directly obtained without the need for phase stepping. Fig. 4.3 shows the holographic interference pattern obtained by the reconstruction of the superposed holograms with and without the flame. One can see the wick of the candle in the reconstruction.

Fig.4. 3: Holographic interference pattern obtained by superposing the holograms recorded with and without the flame.

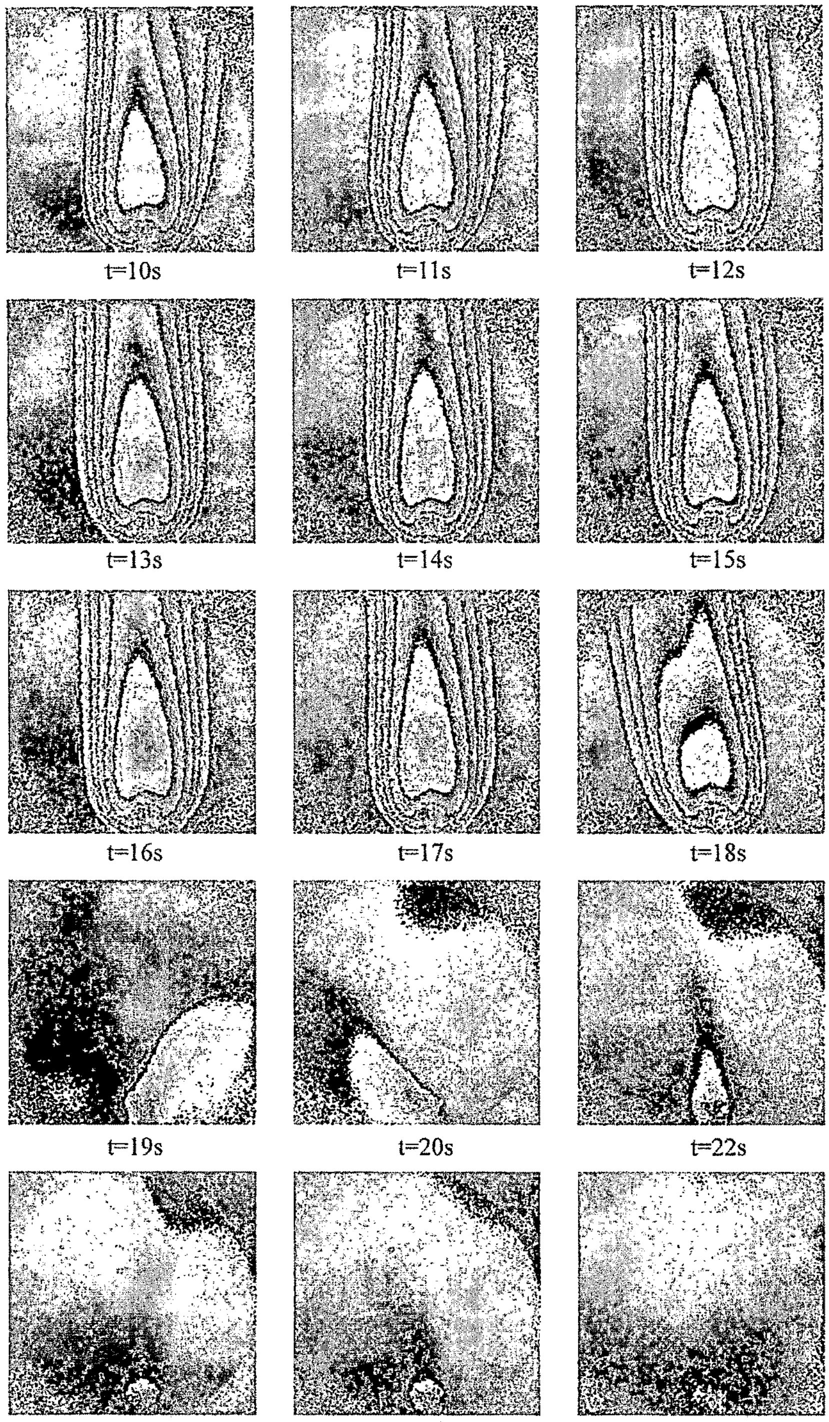

Fig. 4.4: Time evolution of object wavefront phase difference. The flame was turned off after18s.

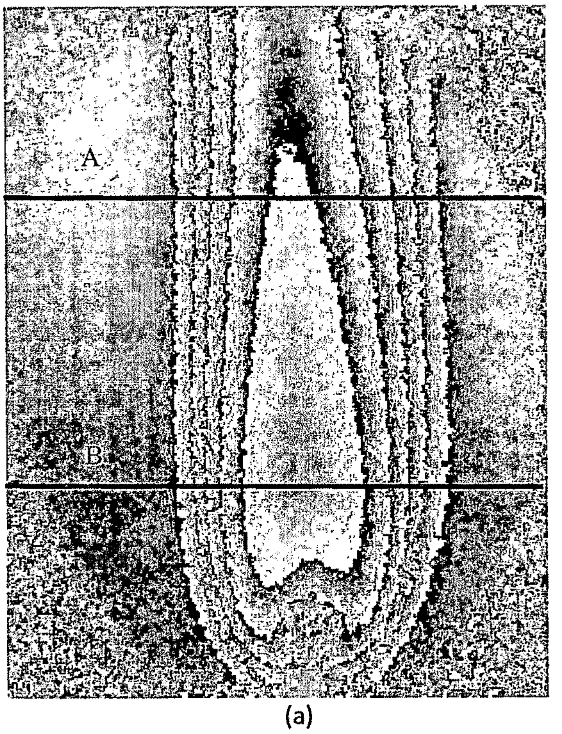

(a)

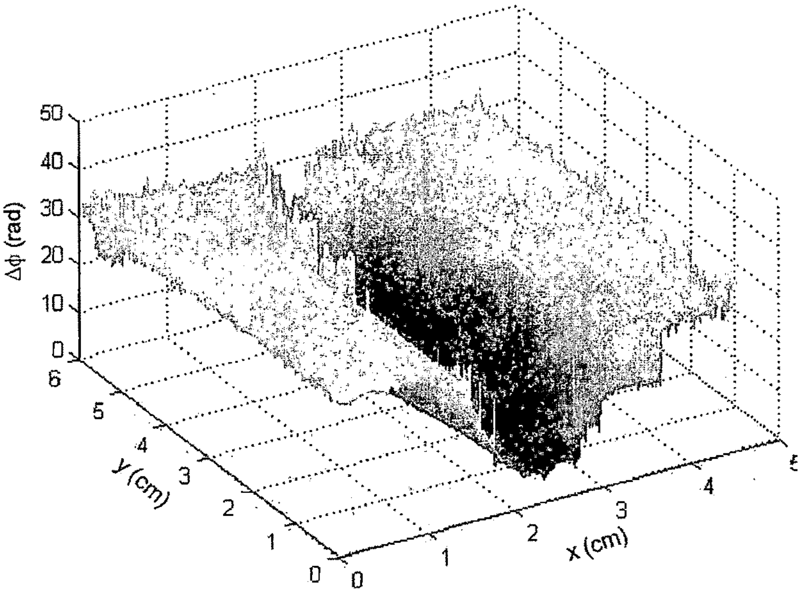

(b)

Fig. 4.5: a) The phase difference incurred by the object beam after 28s due to the existence of the flame calculated using Eq. (15) and (c) The unwrapped phase distribution.

Phases of the individual object states were subtracted to get the phase difference using Eq. (75). The time evolution of the phase difference for the candle flame is shown in Fig. 4.4. This was unwrapped and the unwrapped phase was used for the inversion to get the refractive index profile. Fig 4.5 shows the phase distribution 28 seconds after the candle was lit along with the 3D phase profile after unwrapping. The chord integrated phase difference along the lines A and B in Fig. 4.5b are shown in Fig. 4.6a and 4.6b respectively.

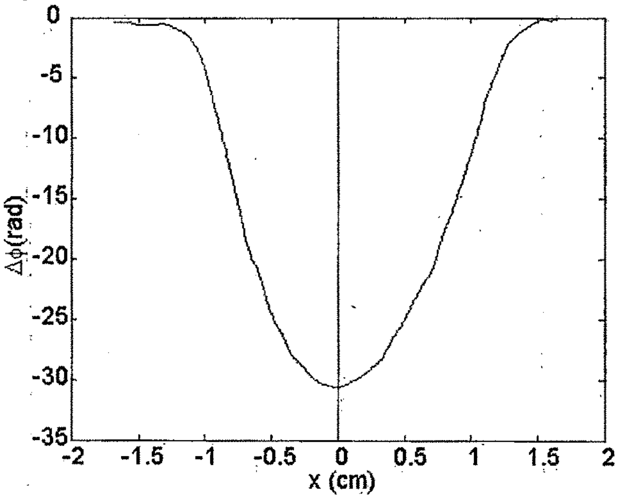

(a)

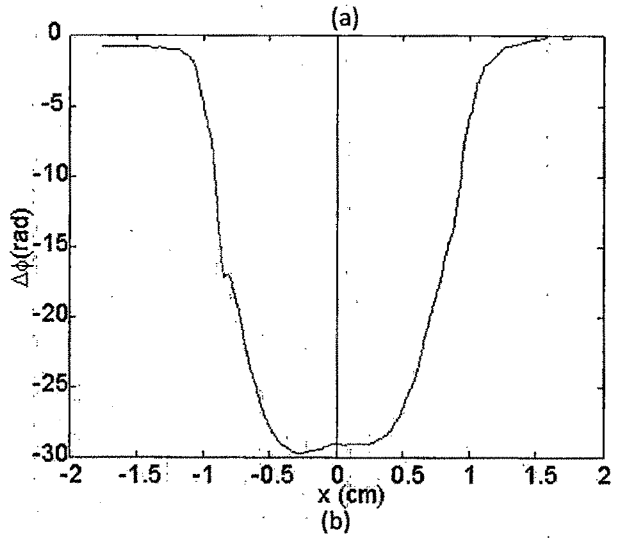

(b)

Fig. 4.6: Chord integrated phase change along (a) line A, (b) line B shown in Fig. 5b.

The left and right portions of the chord integrated values are used for Abel inversion to obtain the refractive index distribution on both sides of the centre of the distribution. The reconstructed refractive index profiles from Abel inversion of the chord integrated values in Fig. 4.6a and4. 6b are shown in Fig. 4.7a and 4.7b respectively. Using the temperature coefficient of refractive index for candle flame, this can be converted into change in temperature (ΔT) with position. Knowing the temperature at any one position, this data can be converted into absolute temperature (T) inside the flame. Here larger the change in refractive index represents larger change in temperature. From the refractive index plots it can be seen that the farther away from the wick of the candle the maximum temperature change occurs at the centre of the flame, where as near the wick, the maximum temperature change does not occur at the centre since the oxygen content near the wick is less resulting in less combustion.

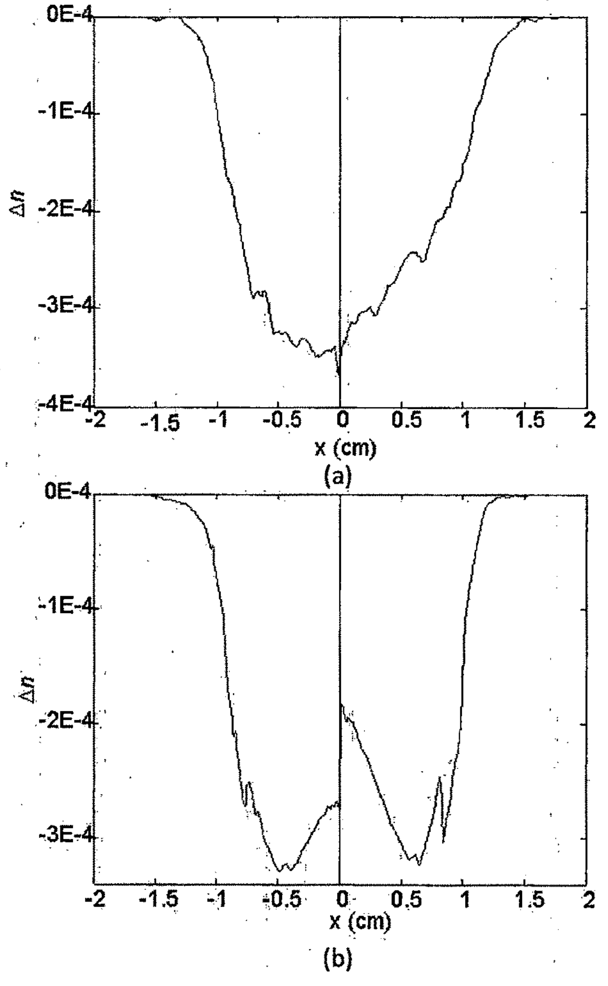

Fig. 4.7: Refractive index distribution obtained by Abel inversion of chord integrated phase values shown in Fig. 6a and 6b respectively.

4.6.2 Temporal evolution of refractive index distribution in a dielectric slab

Heat conduction in dielectric mediums is of great importance from their application point of view. The heat diffusion in such a medium determines its use as a thermal insulator. The heat diffusion is determined from the rate of change of temperature with time for such a medium. So the next set of experiments considered the temporal evolution of refractive index distribution in a dielectric slab when exposed to a point heat source (Fig. 4.8). A flint glass plate of dimensions 8cm×8cm×1cm was used. The laser source and detector were same as the ones mentioned in the previous experiment. Distance between the glass plate and the CCD was 0.8m. The plane object wavefront was passed long the width (1cm) of the slab. The maximum temperature at the glass slab where the point heat source was in touch with the slab was 354K.

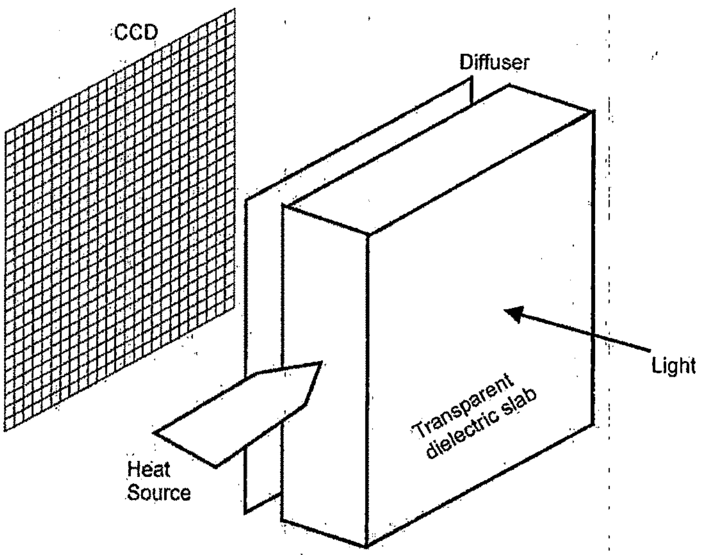

Fig. 4.8: Heating mechanism for the dielectric slab

Holograms were recorded at regular intervals. The phase difference between the initial (when there was no hear source) object state and object after every second after the heat source was switched on were computed. The temporal evolution of the phase change is shown in Fig. 4.9. The heat source was switched off after 150s of heating. From the phase map the diffusion of heat into the system is clearly visible. Also can be seen is that the system has an axis of symmetry about which the tomographic inversion can be performed.

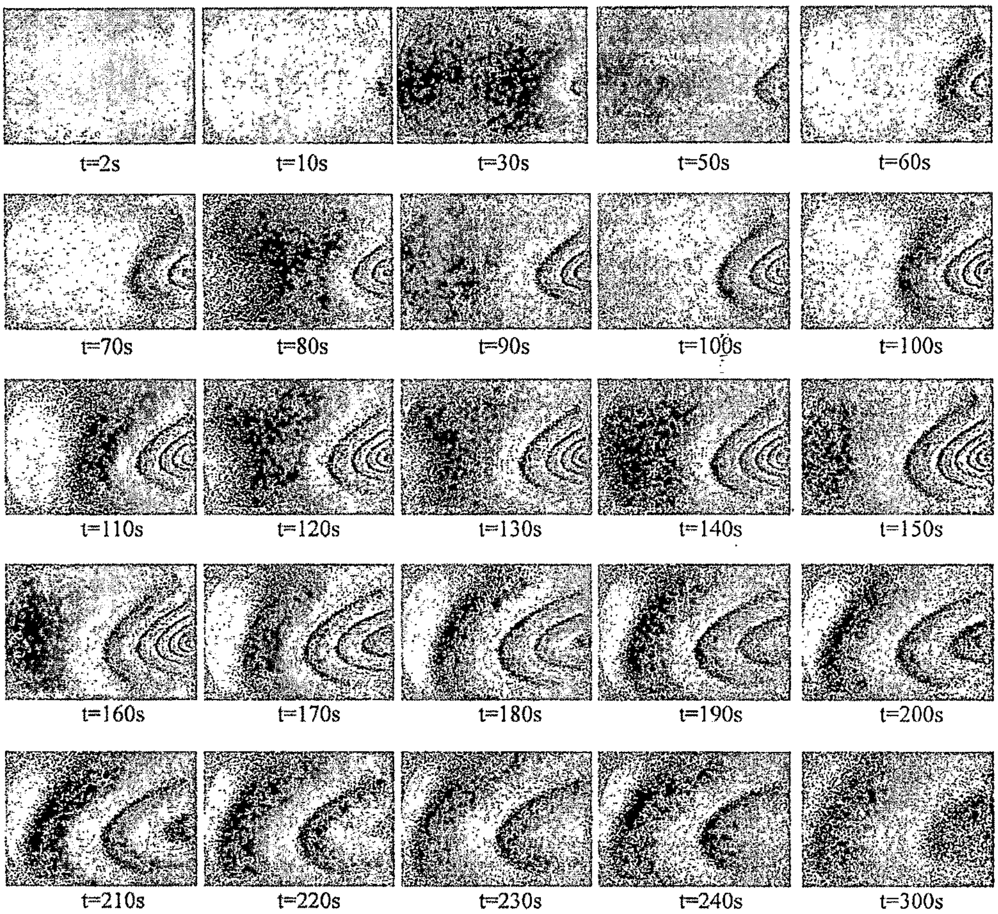

Fig. 4.9: Time evolution of phase difference for thermal diffusion process in a dielectric slab exposed to a point heat source. Maximum temperature of the heat source was 354K. The heat source was turned off after150s.

From the figure it can also be seen that even after the heat source was switched off the diffusion process continues. Fig. 4.10 shows the phase maps at time instances 50s, 100s and 150s respectively after the heat source was switched on. The unwrapped phase maps corresponding to them are shown in Fig. 4.11. They were used for tomographic inversion to obtain the refractive index variation.

(a) (b) (c)

Fig. 4.10: Phase difference as a function of time (a) after 50s (b) after 100s (c) after 150s. Abel inversion was performed along the line shown in Fig. 10a.

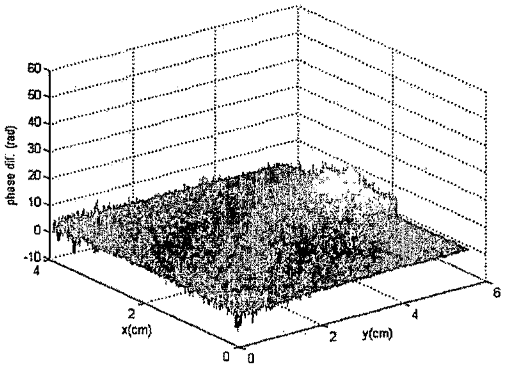

(a)

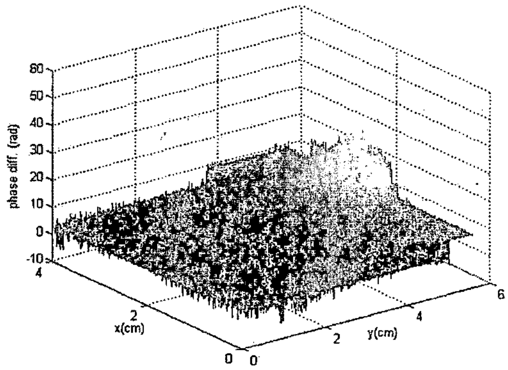

(b)

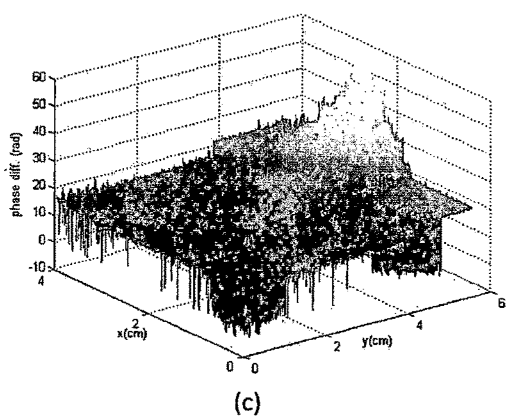

(c)

Fig. 4.11: Unwrapped phase maps corresponding to Fig. 10a, 10b and 10c respectively

The chord integrated phase change along the line shown in Fig. 4.10a for three time instances is given in Fig. 4.12. Here also the left and right part of the centre (symmetry axis) is used for Abel inversion.

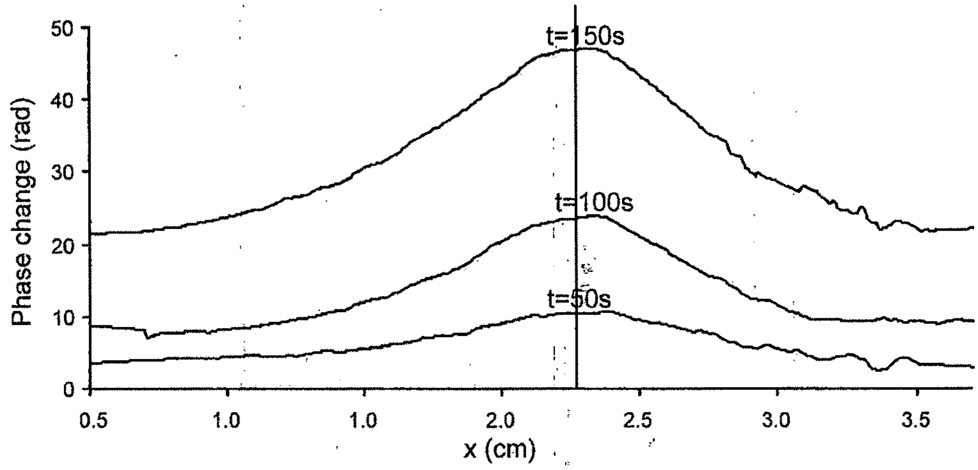

Fig. 4.12: Chord integrated phase difference along the line shown in Fig. 10a

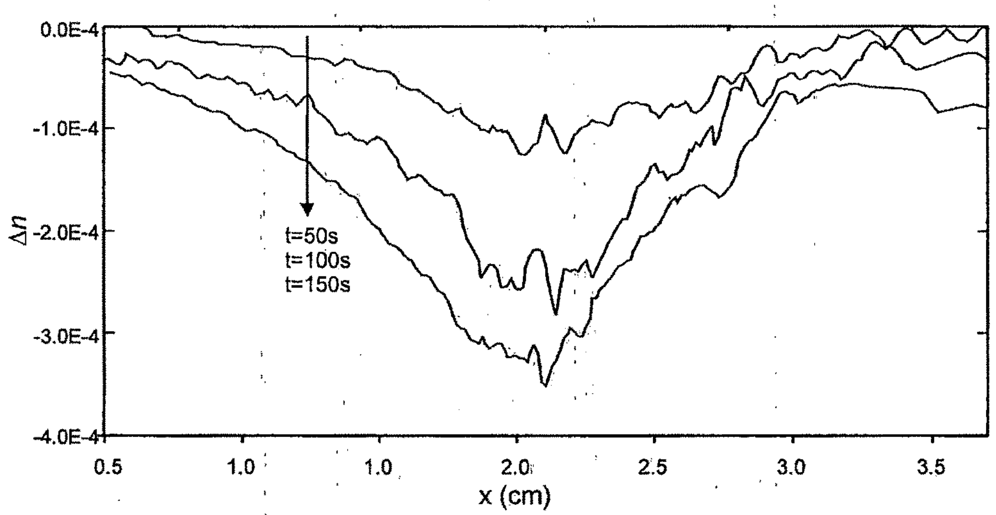

Fig. 4.13: Time evolution of refractive index distribution inside the glass slab obtained by Abel inversion of the chord integrated values shown in Fig, 12

The refractive index change obtained from Abel inversion is depicted in Fig. 4.13. In this case the maximum change of temperature occurs at the centre. This is because the source was pointed and placed along the axis of symmetry.

4.6.3 Temperature distribution in air using a point heat source

For refractive index distributions occupying small volumes, the experimental setup can be made compact by keeping the detector near to the object. Angular spectrum propagation integral can be use for reconstructions. Reconstruction using angular spectrum propagation integral was investigated in the case of a temperature distribution produced in air by a point source. Here a 633nm He-Ne laser was used as the source. Object was kept at a distance of 10cm from the detector which was a CCD camera having 1024×1024 pixels with pixel size 9.8μ×9.8μ having 8-bit dynamic range. The object and the propagation directions of the probe beam are shown in Fig. 4.14.

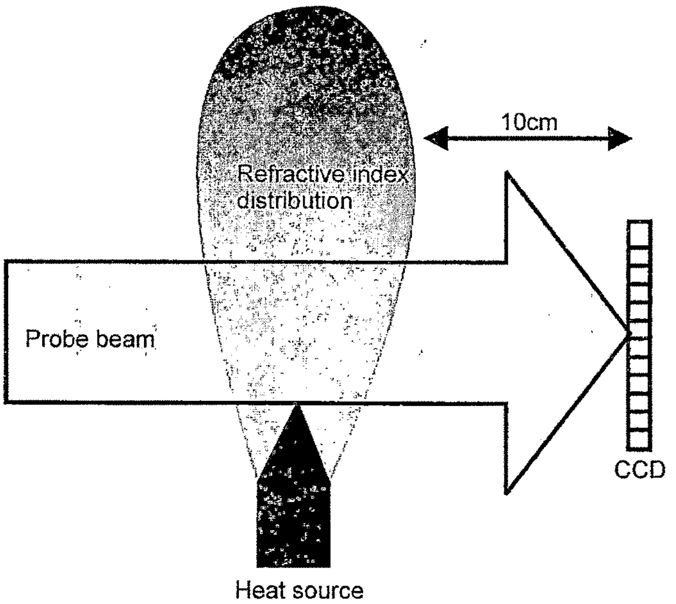

Fig. 4.14: Pointed heating element producing a refractive index distribution in air. The Probe laser beam used in this case had vacuum wavelength of 633nm and power of 15mW.

The reconstructions were performed using the method described in Section 8 of Chapter2. For reconstructions using angular spectrum propagation, reconstructed pixel size is same as the detector pixel size. So the object dimensions that can be imaged are same as that of the detector dimensions. Fig. 4.15a shows the obtained phase difference after 10s of switching on the heat source. The unwrapped phase distribution is used for determining the refractive index distribution. Fig. 4.15b depicts the reconstructed refractive index profile along the line horizontal shown in Fig. 4.15a.

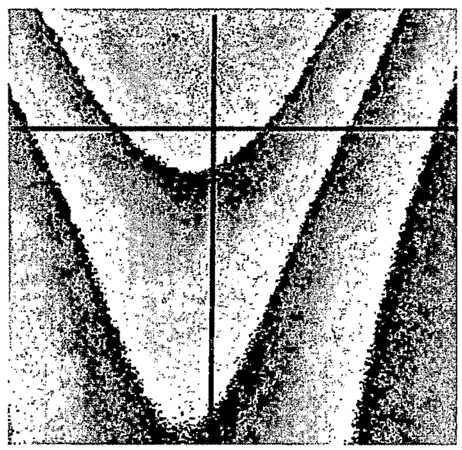

(a)

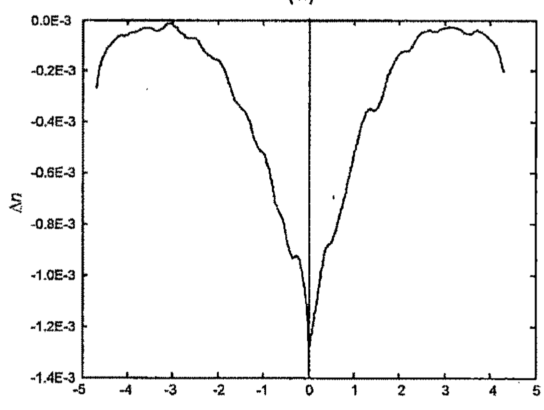

(b)

Fig. 4.15: (a) Computed phase difference 10s after the heat source was switched on. (b) The reconstructed refractive index profile along the horizontal line shown in Fig. 15a

The refractive index profile for the whole object can be reconstructed by Abel inversion along all the horizontal lines, where the chord integrated data is available. These can be put together to obtain the refractive index distribution along any plane. Fig. 4.16 shows the obtained refractive index distribution along the horizontal line (x-z plane) in Fig. 4.15a. Fig. 4.17 shows the obtained refractive index distribution along the vertical line (x-y plane) shown in Fig. 4.15a.

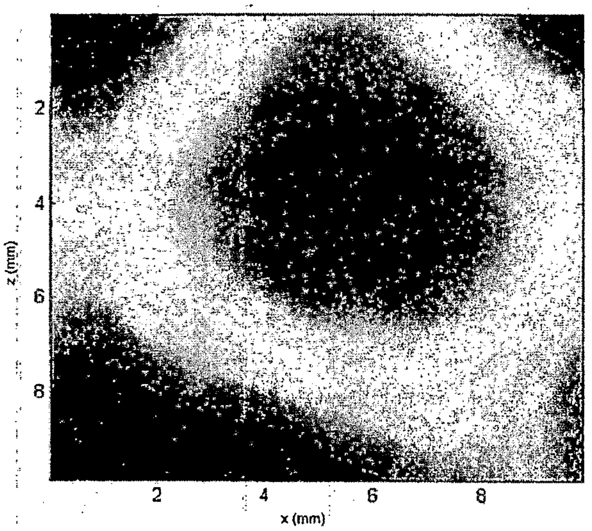

Fig. 4.16: Computed refractive index distribution along the x-z plane

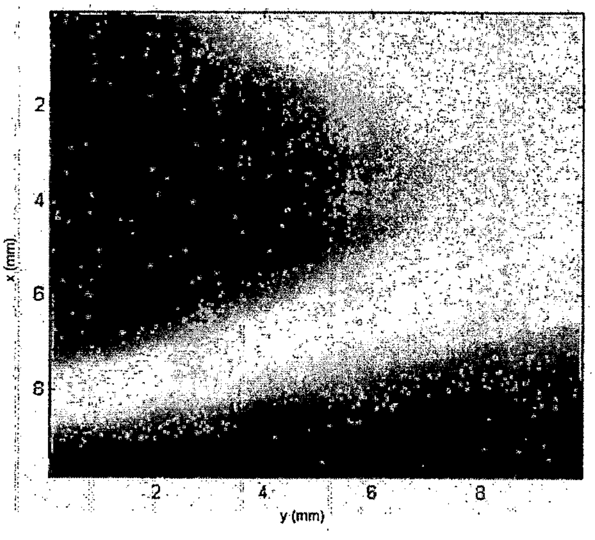

Fig. 4.17: Computed refractive index distribution along the x-y plane

4.7 Discussions and Conclusion

A method for mapping refractive index distribution and to investigate temperature profile of phase objects using digital holography has been developed. Digital holographic interferometry along with Abel inversion was used was used for this. The phase of the object wavefront was obtained directly from the reconstructed complex amplitude. The phase difference with and without the object distribution is used to tomographically reconstruct the refractive index profile. The principle behind the system is the path difference of the beam caused by refractive index change.

Experimental results confirm that this method can be applied to investigate tomographically the spatially as well as temporally varying refractive index distributions in axi-symmetric transparent phase objects. Simple Abel inversion yields the refractive index profile from the chord integrated phase obtained after the hologram reconstruction. With the use of a diffuser in front of the phase objects the method could be utilized to investigate large objects. The role of the diffuser is to make sure that information from the whole object reaches the detector plane. Fresnel transform was used in reconstructions and the reconstructed pixel size changes with the reconstruction distance. But in the case of smaller objects the angular spectrum propagation integral was used to reconstruct the hologram. Here the pixel size at the reconstruction plane remains same as the detector pixel size. The main advantage of this method is that it can separate out the spectrum due to the object alone and hence the overlap between the virtual image, real image and un-diffracted reference beam at the reconstruction plane is avoided. Slowly evolving refractive index distributions like that in the glass slab could be investigated with the method. Rapidly evolving phenomena could be investigated with the same method using fast CMOS detectors available today. The method will be useful in investigating gas plumes, probing transparent dielectric materials for their heat transfer properties and for investigating laser produced plasma as well as jets. Since refractive index depends upon various parameters inside the phase medium like its temperature distribution, density distribution, impurity distribution etc., this method can also be used to determine these factors. With some modifications the method could also be made quasi real-time to yield refractive index distributions, which could be used as a feed back control in several applications like vacuum coating systems, laser produced plasma for extreme ultraviolet generation, control of gas jets etc.

References

[4.1] Hutchinson, I. H., [Principles of plasma diagnostics], Cambridge University Press, Cambridge (2002).

[4.2] Muraoka, K. and Maeda, M., [Laser-aided diagnostics of plasmas and gases] IOP publishers, Bristol (2001).

[4.3] Ostrovskaya, G. V., Butosov, M. M. and Ostrovsky, Y. I. [Interferometry by holography] Springer-Verlag, Berlin (1980).

[4.4] Kreis, T., [Hand Book of Holographic interferoemtry] Wiley-VCH, Weinheim (2005).

[4.5] Sweeney, D. W. and Vest, C. M., "Reconstruction of Three-Dimensional Refractive Index Fields by Holographic Interferometry", Appl. Opt. **11**, 205 (1972).

[4.6] Sweeney, D. W. and C. M. Vest, "Reconstruction of Three-Dimensional Refractive Index Fields from Multidirectional Interferometric Data", Appl. Opt. **12**, 2649 (1973).

[4.7] Cha, S. and Vest, C. M., "Interferometry and reconstruction of strongly refracting asymmetric-refractive-index fields", Opt. Lett. **10**, 311(1979).

[4.8] Vest, C. M., "Interferometry of strongly refracting axisymmetric phase objects", Appl. Opt. **14**, 1601 (1975).

[4.9] Jackson, S. L. and Shumlak, U., "Abel inversion of a holographic interferogram for determination of the density profile of a sheared-flow Z pinch", Rev. Sci. Instrum. **77**, 083502 (2006).

[4.10] Schnars, U. and Juptner, W., "Digital recording and numerical reconstruction of holograms", Meas. Sci. Technol. **13**, R85-R101 (2002).

[4.11] Kim, M. K., Yu, L. and Mann, C. J., "Interference techniques in digital holography", J. Opt. A: Pure Appl. Opt. **8**, S518 (2006).

[4.12] A. Anand, V. K. Chhaniwal, G. Pedrini, W. Osten, " Digital holographic tomography of phase objects", Proc. SPIE, **7389**, 73890L (2009).